Optomechanical spectroscopy with broadband interferometric and quantum cascade laser sources

L. Tetard,[1] A. Passian,[1,2,*] R. H. Farahi,[1] B. H. Davison,[1] and T. Thundat[1]

[1]*Oak Ridge National Laboratory, Oak Ridge, Tennessee 37831-6123 USA*

[2]*Department of Physics, University of Tennessee, Knoxville, Tennessee 37996, USA*

**Corresponding author: passianan@ornl.gov*

Received May 12, 2011; revised July 3, 2011; accepted July 9, 2011;
posted July 28, 2011 (Doc. ID 147450); published MONTH 0, 0000

The spectral tunability of semiconductor–metal multilayer structures can provide a channel for the conversion of light into useful mechanical actuation. Responses of suspended silicon, silicon nitride, chromium, gold, and aluminum microstructures are shown to be utilized as a detector for visible and IR spectroscopy. Both dispersive and interferometric approaches are investigated to delineate the potential use of the structures in spatially resolved spectroscopy and spectrally resolved microscopy. The thermoplasmonic, spectral absorption, interference effects, and the associated energy deposition that contributes to the mechanical response are discussed to describe the potential of optomechanical detection in future integrated spectrometers.

OCIS codes: , .

Manipulations of materials at the structural levels or via bandgap engineering provide a means to achieve many fascinating phenomena, ranging from filtering exhibited by stratified materials [1] to negative refraction exhibited by metamaterials [2–4]. Applications are equally intriguing and diverse, such as plasmonic enhancement [5], cloaking [6,7], and invisibility [8]. Recently, optomechanics has also emerged as a means to manipulate mesoscopic systems [9,10] by taking advantage of electromagnetic–mechanical couplings involving photothermal, radiation pressure [11], and stochastic forces [12]. Notable among these is the formation of an optical interferogram (e.g., in a Michelson interferometer), with important applications in spectral measurements of the molecular signatures of materials and spatial measurements of subnanometer displacements. These capabilities have been at the core of developing the Fourier transform IR (FTIR) spectrometer, gravitational wave detector [13], and laser Doppler vibrometers [14]. As a result, the optical interaction with microstructures continues to attract study, such as analyzing the transport of photogenerated carriers [15] or the observation of Fano-like resonances [16]. The optical response of the typical atomic force microscope (AFM) silicon (Si) or silicon nitrite (Si_3N_4) probes, the microcantilevers [17], in conjunction with the introduction of various nanophotonic and waveguide structures [18], indicate their potential application as nanomechanical spectrometers. Furthermore, due to the ease of interfacing microstructures with noble metal thin films and nanostructures, thermoplasmonic and other plasmonic processes [19] can be capitalized upon as new actuation mechanisms. In this Letter, by investigating (1) an optomechanical interferogram and (2) the photothermal response of micromechanical structures to mid-IR lasers, we introduce the concept of Fourier transform optomechanical spectroscopy (FTOS).

The experimental arrangement is shown in Fig. 1. A broadband source (1.5–25 μm) and a tunable pulsed quantum cascade laser (QCL) [20] (9.25–9.81 μm) provide radiation that can interact with a series of metal-coated AFM cantilevers. The core components of a typical (1) interferometric measurement intended to demonstrate FTOS with oscillator C_1, (2) dispersive measurement on C_2, and (3) deflection measurement on C_3 are shown in Fig. 1. Noting that measurement (3) is used to read out the deformation of a probe, it is clear that such arrays of oscillators may be integrated for specific applications in optomechanics [21]. Data were obtained by angle controlled illumination and optical deflection detection using a dimensional and a multimode AFM system. Focusing a collimated 1 in. (2.54 cm) diameter broadband beam (Spectrum GX, Perkin Elmer), we characterized the resonators in the range of 1.5–25 μm and compared the

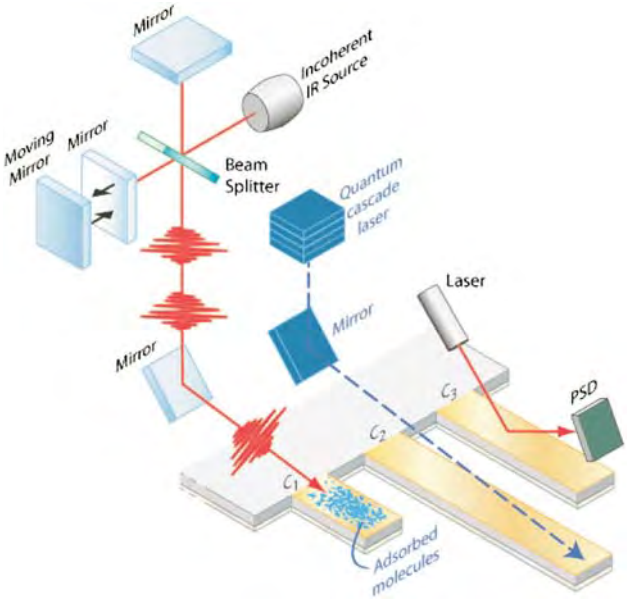

Fig. 1. (Color online) Optomechanical spectrometer based on an array of microstructures C_i, $i = 1, 2, \ldots$. The pulses indicate the interferometer operation (left) and the quantum cascade laser (middle). The right laser and the PSD detect the state of the cantilevers.

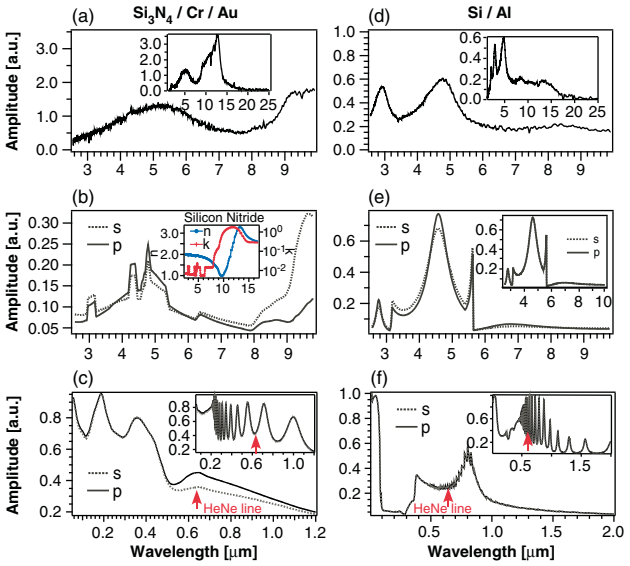

Fig. 2. (Color online) Optomechanics of (a)–(c) Au–Si_3N_4 and (d)–(f) Al–Si AFM probes. Spectra for incidence at the semiconductor layer in (a), (b), (d), and (e) and the insets of (c), (f), with the data in the mid-IR in (a) and (d), and the theoretical s and p polarization (incidence 30°) absorption in (b) and (e). Insets (a) and (d) show the 1.5–25 μm spectra, while the case of 0° is shown in inset (e). The inset in (b) shows the properties of Si_3N_4 [22]. In (c) and (f), the responses in the visible and near-IR are presented when the metal layer is exposed, while the insets show the semiconductor exposure. Arrows indicate the He–Ne line used in the oscillation detection of the probe.

results with theory in Fig. 2. The data were collected by averaging at a 4 cm^{-1} resolution. Spectra from Au–Si_3N_4 and Al–Si probes are shown in Figs. 2(a)–2(c) and Figs. 2(d)–2(f), respectively, and Fig. 3. To further analyze the data acquired from the studied probes C_i, we simulated the optical response of their material domains. The agreement between the data in Figs. 2(a) and 2(d) and the simulations in Figs. 2(b) and 2(e) is good, apart from the dissipative features of the Si_3N_4, as seen from the dielectric function (n, k) [22] in the inset of Fig. 2(b). From the results in Figs. 2(b), 2(c), 2(e), and 2(f), one may identify the absorption bands: N–H bending at 8.93 μm, and the stretching of Si–N at 10.87 and 12.20 μm, Si–H at 4.61 μm, and N–H at 2.99 μm [22].

The measurements can be extended to the dynamic range where amplitude modulated lasers may be used to resonantly excite the eigenmodes of the probe. Characterization of the optomechanical response using the QCL (center wavelength $\lambda = 9636$ nm) is shown in Fig. 3, where the beam is pulsed at frequency f_p (tunable from a few hertz to 100 kHz) with pulse width W_p (tunable from 0.02 to 0.5 μs) and current A (tunable from 800 mA to 1 A). Scanning the pump QCL at the beam waist, over a mesh of $(\Delta x, \Delta y) = (15, 12.7)$ μm, the cantilever spatially profiles the incident beam, as shown by the lock-in measurement of the readout laser in Figs. 3(a) and 3(b), acquired for $f_p = 10.2$ kHz (corresponding to the first resonance of the probe) and with maximum A and W_p. In Figs. 3(c) and 3(d), the lock-in measures the response to f_p and W_p of the QCL. In Fig. 3(c), the contribution of the laser to the Brownian motion of the microcantilever was evaluated by measuring the position sensitive detector

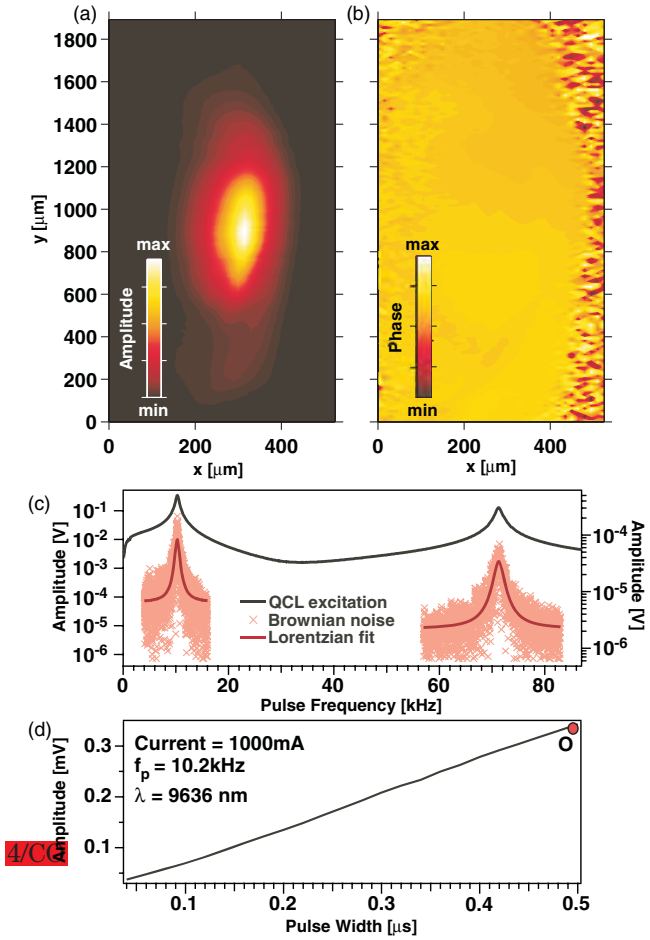

Fig. 3. (Color online) (a) Amplitude and (b) phase of the QCL beam profile measured with an Al–Si microcantilever ($k = 0.03$ N/m). Probe's response to (c) f_p and (d) W_p of the QCL output obtained by lock-in measurement. The two data sets and their numerical fits in (c) show the noise excited resonances of the probe. O, in (d), is the operational point used in (c) with $f_p = 100$ kHz.

(PSD) signal via a lock-in internal reference sweep. The lowest state Brownian noise with the laser off, shown in symbols and fitted in red, is superimposed with the Brownian noise in the case when the laser delivers the most energy to the microcantilever at $f_p = 100$ kHz, $A = 1$ A, and $W_p = 0.50$ μs. As the results show, the increase in thermal noise due to the laser itself is negligible. Figure 3(d) indicates the linear dependence of the optomechanical response of the microcantilever at resonance with respect to W_p. We note that, since the low power He–Ne beam is not modulated and, from Fig. 2(f), it contributes only a small fraction to the heating of the probe, it will not cause any coupling with the motion due to the pump beam. Seen from the pump beam, the cantilever motion may present an oscillation in the angle of incidence, which by comparison of Fig. 2(e) and its inset, is deemed negligible.

The FTOS data in Fig. 2 is a result of a fast Fourier transform (FFT) of the optomechanical interferogram generated by the PSD in Fig. 1, whereas Fig. 3 represents the output of the PSD in response to the pulsed QCL. In both cases, the force distribution within the probe $w(x, t)$ is directly related to the spectral absorption of the

electromagnetic energy in the material layers. This Poynting energy forms the source term for the heat equation that can be solved for the specific boundary conditions of the structure to yield the transient temperature distribution $T(x,t)$. Consequently $T(x,t)$ leads to a deformation $d(x,t)$ as a result of the asymmetric thermal expansion (each material layer possessing a different thermal expansion coefficient). Thus, for a fixed velocity v of the moving mirror in Fig. 1 yielding an optical path difference (OPD) of $\delta = 2vt$, the signal from the PSD can be expressed as a function of time t as $S(t) = \int_0^\infty S(\nu)\cos(4\pi vt)\nu \mathrm{d}\nu$, where $S(\nu)$ is proportional to the responsivity of the probe and the amplifier as a function of wavenumber ν. Since $S(t) \propto d(x,t)$ (within an electronic amplification factor and calibration), we can solve for the transient probe response and obtain $d(x,t) = \sum_{k=1}^{\infty} \Phi_k(x) g_k(t) \omega_k^{-1}$, where $\Phi_k(x)$ is the kth eigenmode of the probe (eigenfrequency ω_k) and

$$g_k(t) = \int_0^1 \Phi_k(u)\mathrm{d}u \int_0^1 w(u,\tau) e^{-\eta(t-\tau)} \sin\omega_k(t-\tau)\mathrm{d}\tau,$$

while $w(u,\tau)$ represents the bulk force [12] and η is related to the damping. Note that, with a proper apodization applied to $S(t)$ when processed for the FFT, the spectral resolution of FTOS is related to both the maximum OPD of the scan and the response time of the probe. Since the modulation frequency of the interferogram is proportional to ν and v, we obtain, for $v = 1\,\mathrm{cm}\cdot\mathrm{s}^{-1}$ and wavenumber of $4000\,\mathrm{cm}^{-1}$, a frequency of 8 kHz, which is well within the response time of all the probes used (compared with the lowest lying resonances of 10.2 and 22 kHz for the Si–Al and Si_3N_4–Cr–Au probes). Comparing the interferograms obtained using the FTOS with those generated by the standard KBr detector of the FTIR, we established that FTOS readily resolves the fastest variation in amplitude.

We conclude that optomechanical systems can provide spectrally resolved detection of radiation and thus be integral parts of microspectrometers. Advances in metrology and sensing demand an understanding of the optomechanical properties of novel actuators, particularly for high resolution imaging and detection. The optical response must be catered accordingly, depending upon whether the structure is to be used in a direct chemical/biological sensing application, that is, responding to the transfer of the thermal absorption energy from the sample in contact with the structure, or in the measurement of the scattered light from the sample, that is, a direct photothermal scheme. The presented spectra show that both the interferometric and single beam parameters can trigger various couplings between the elastic, the optical, and the thermo-optic responses. While any thermoelastic dissipation and potential Fano-like structures are implicit in our dynamic (QCL) measurements of the Q-factor and the form of the resonance lines, they appear of little or no consequence in the interferometric measurements, strengthening the potential of FTOS for high resolution spectroscopy. We introduced the concept of thermoplasmonic actuation via the nonradiative decay of surface plasmons that can provide a significant channel for energy deposition.

This research was sponsored in part by the Oak Ridge National Laboratory (ORNL) BioEnergy Science Center (BESC) and laboratory directed research and development (LDRD) fund. BESC is a U.S. Department of Energy (DOE) Bioenergy Research Center supported by the Office of Biological and Environmental Research in the DOE Office of Science. ORNL is managed by UT-Battelle, LLC, for the U.S. DOE under contract DE-AC05-00OR22725.

References

1. M. Gerken and D. A. B. Miller, Appl. Opt. **42**, 1330 (2003).
2. D. R. Smith and N. Kroll, Phys. Rev. Lett. **85**, 2933 (2000).
3. R. A. Shelby, D. R. Smith, and S. Schultz, Science **292**, 77 (2001).
4. J. Valentine, S. Zhang, T. Zentgraf, E. Ulin-Avila, D. A. Genov, G. Bartal, and X. Zhang, Nature **455**, 376 (2008).
5. H. J. Lezec, J. A. Dionne, and H. A. Atwater, Science **316**, 430 (2007).
6. J. B. Pendry, D. Schurig, and D. R. Smith, Science **312**, 1780 (2006).
7. D. Schurig, J. J. Mock, B. J. Justice, S. A. Cummer, J. B. Pendry, A. F. Starr, and D. R. Smith, Science **314**, 977 (2006).
8. U. Leonhardt, Science **312**, 1777 (2006).
9. T. Rocheleau, T. Ndukum, C. Macklin, J. B. Hertzberg, A. A. Clerk, and K. C. Schwab, Nature **463**, 72 (2010).
10. A. Nunnenkamp, K. Børkje, J. G. E. Harris, and S. M. Girvin, Phys. Rev. A **82**, 021806 (2010).
11. M. Eichenfield, J. Chan, R. M. Camacho, K. J. Vahala, and O. Painter, Nature **462**, 78 (2009).
12. A. Passian, A. Lereu, D. Yi, S. Barhen, and T. Thundat, Phys. Rev. B **75**, 233403 (2007).
13. P. Aufmuth and K. Danzmann, New J. Phys. **7**, 202 (2005).
14. B. Ohler, Rev. Sci. Instrum. **78**, 063701 (2007).
15. D. M. Todorovic, B. Cretin, Y. Q. Song, and P. Vairac, J. Appl. Phys. **107**, 023516 (2010).
16. S. Kadri, H. Fujiwara, and K. Sasaki, Opt. Express **19**, 2317 (2011).
17. A. Wig, E. Arakawa, A. Passian, T. Ferrell, and T. Thundat, Sens. Actuators B **114**, 206 (2006).
18. J. W. Noh, R. Anderson, S. Kim, J. Cardenas, and G. P. Nordin, Opt. Express **16**, 12114 (2008).
19. A. L. Lereu, A. Passian, R. H. Farahi, N. F. van Hulst, T. L. Ferrell, and T. Thundat, J. Vac. Sci. Technol. A **26**, 836 (2008).
20. J. Faist, F. Capasso, D. L. Sivco, C. Sirtori, A. L. Hutchinson, and A. Y. Cho, Science **264**, 553 (1994).
21. F. Marquardt and S. Girvin, Physics **2**, 40 (2009).
22. M. Klanjsek Gunde and M. Macek, Phys. Status Solidi A **183**, 439 (2001).

Queries

1. Please provide two to six OCIS codes from http://www.opticsinfobase.org/submit/ocis/
2. SI equivalents are typically given for English measurements. Is 2.54 cm okay for 1 in.?
3. Please check the references to Figs. 2(f) and 2(e) in the last two sentences of this paragraph. Are these correct?